

Light charged particle evaporation from hot ^{31}P nucleus at $E^* \sim 60$ MeV

D. Bandyopadhyay, C. Bhattacharya, K. Krishan, S. Bhattacharya, S. K. Basu
Variable Energy Cyclotron Centre, 1/AF Bidhan Nagar, Kolkata - 700 064, India

A. Chatterjee, S. Kailas, A. Shrivastava, K. Mahata
Nuclear Physics Division, Bhabha Atomic Research Centre, Mumbai - 400 085, India

Abstract

The energy spectra of evaporated light charged particles, such as, α , p, d and t, have been measured in ^7Li (47 MeV) + ^{24}Mg and ^{19}F (96 MeV) + ^{12}C reactions. The data have been compared with the predictions of the statistical model code CASCADE. It has been observed that the spectra obtained in the ^7Li (47 MeV) + ^{24}Mg reaction follow the standard statistical model prediction with a spherical configuration of the compound nucleus. But, the spectra obtained in the ^{19}F (96 MeV) + ^{12}C reaction deviate from similar predictions of the statistical model both on higher as well as on lower energy sides. Considerable deformation was required to modify the transmission probabilities and the available phase spaces in order to reproduce the measured energy spectra in this case. Dynamical trajectory model calculations were not very successful to explain the differences in behaviour in the decay of compound nucleus (^{31}P), formed through the two entrance channels under study, in terms of the comparable formation and decay times. The observed discrepancy has been attributed to the effect of larger input angular momentum in case of ^{19}F (96 MeV) + ^{12}C system.

I. INTRODUCTION

In recent years, there has been a lot of interest to study the statistical properties of hot rotating nuclei populated at high angular momenta and excitation energies [1–4]. It is possible to produce an appreciably deformed compound nucleus with high angular momentum and excitation energy through heavy ion fusion reactions. High excitation energy favours the compound nucleus to deexcite through the statistical emission of several light particles followed by γ decay. The statistical decay implies that the compound nucleus has lived long enough making all the decay channels equally probable. The decay process is governed by the available phase spaces, *i.e.*, the nuclear level densities of both the parent and daughter nuclei, as a function of excitation energy, angular momentum and deformation. The evaporated light charged particle spectra in conjunction with the statistical model calculations can be used to extract the statistical properties of the equilibrated compound system.

However, recent studies show that at high excitation energies and angular momenta, the energy spectra of evaporated light charged particles, are no longer consistent with the statistical model predictions. A large number of experiments have been performed in last few years to study this anomaly over a wide range of compound nuclear masses A_{CN} in the range of \sim 60–170, for example [1–10], and in most cases it has been found that the statistical model fail to explain the observed light charged particle energy spectra. Choudhury et al [5] have measured the α -particle energy spectra in the reaction 214 MeV ^{32}S on ^{27}Al and observed that the measured spectra deviate considerably from the standard statistical model predictions. Rana et al [6] have measured α -particle spectra in the reaction 190 MeV ^{40}Ar on ^{27}Al and have seen similar discrepancy. The authors argued that in the statistical model calculation, the emission barrier is considered as the fusion barrier of the two partners in the exit channel assuming their spherical configuration. It may be a good approximation at low excitation energy and angular momentum. But, when the nucleus is at high excitation energy and rotating with high spin, it is likely to be deformed in shape rather than being spherical. Hence, the emission barrier will be lower if we consider that the α -particles are emitted preferentially along the larger axis. On the contrary, Govil et al [7] and Huizenga et al [8] have claimed that the anomaly may be well explained by incorporating spin dependent level density in the standard statistical model prescription to modify the yrast line keeping the emission barrier unchanged. According to them, only deformation, unless it is unrealistically large cannot affect the α -particle emission barrier much. Recently, Charity et al [10] have measured light charged particle spectra emitted in the reactions ^{64}Ni on ^{100}Mo and ^{16}O on ^{148}Sm and have shown that not only the measured spectra deviate from the statistical model predictions but the magnitude of the deviation also depends on the excitation energy and the entrance channel. According to them, for incident energies below 5 MeV/A, the experimental results agree well with the theoretical predictions. However, above 5 MeV/A, the experimental results show significant deviation from the calculated spectra. Intuitively, the shape of the light charged particle spectra would

be affected by the deformation of the equilibrated system if it remains deformed over a time scale comparable to the mean lifetime of charged particle emission. Recently, Govil et al have measured the α -particle energy spectra emitted in 83, 97 MeV ^{12}C on ^{45}Sc [2] and 110 MeV ^{16}O on ^{54}Fe [1] reactions. They have shown that the entrance channel dynamics plays a significant role in the decay of compound nucleus. Moreover, Charity et al have shown that the different set of parameters are required for different evaporated light charged particles, such as, α , proton, deuteron and triton [10] to reproduce the experimental data. However, it is interesting to note that Namboodiri et al [11] have measured α -particle emission in the reaction 120 MeV ^{20}Ne on ^{27}Al but did not observe any discrepancy with the statistical model predictions.

It is thus apparent that there exist some discrepancy between the experimentally measured spectra and the corresponding predictions of standard statistical model which is prominent for higher spin and for heavier systems ($A \geq 60$). However, due to lack of experimental data situation is not clear for the lighter systems at relatively lower spin. This prompted us to explore the scenario for light system, such as, ^{31}P , in the incident energy range below 5 MeV/A. There may be some entrance channel effect in the evaporative light particle decay if the nucleus lives in the dinucleus form for a long time and evaporates during this period. But our previous studies on the intermediate mass fragment emission do not reflect the existence of any such long-lived dinuclear configuration [18,19] of the compound nucleus. We have measured α -particles in coincidence with the evaporation residues in the 96 MeV ^{19}F on ^{12}C reaction [12] and have observed that the measured spectra deviate from the theoretical prediction of the statistical model at low as well as at high energy sides. Assuming a deformed configuration of the compound nucleus the full energy spectra could be explained satisfactorily. However, as stated earlier, it would be interesting to explore whether the deformation is linked with the entrance channel dynamics of the system or not. Hence, we have populated the same compound nucleus ^{31}P at similar excitation energy of ~ 60 MeV but through different entrance channels, i.e., 96 MeV ^{19}F on ^{12}C and 47 MeV ^7Li on ^{24}Mg . Since the two reaction channels populate the similar compound system with different angular momentum distributions ($l_{cr} \sim 21 \hbar$ and $16 \hbar$, respectively), it offers an opportunity to study the angular momentum dependence in the evaporative decay cascade. It has been observed by most of the earlier workers, that different amount of deformation is required to explain the different light charged particles data consistently. It directly points to the inadequacy of the standard statistical model to explain the light charged particle emission at higher spin and excitation energies. In order to explore the scenario of light charged particle emission further from a lighter system at moderate spin and excitation energy, we have measured the energy and angular distributions of all the light charged particles, (i.e., α , p, d and t) emitted from excited ^{31}P nucleus, produced by the reactions 96 MeV ^{19}F on ^{12}C and 47 MeV ^7Li on ^{24}Mg .

The paper has been arranged as follows. The experimental details alongwith the experimental results are described in Sec. II. The predictions of the statistical model for ^{31}P nucleus have been discussed in Sec III. Finally the summary and conclusions are presented in Sec IV.

II. EXPERIMENTS AND RESULTS

The experiments were performed at the Bhabha Atomic Research Centre - Tata Institute of Fundamental Research 14 UD pelletron accelerator laboratory, Mumbai, with 96 MeV ^{19}F beam on $125\mu\text{g}/\text{cm}^2$ self-supporting ^{12}C target and 47 MeV ^7Li beam on $275\mu\text{g}/\text{cm}^2$ self-supporting ^{nat}Mg target. The beam current was typically 20-80 nA. The light charged particles have been detected in three solid state telescopes. The telescopes (T_1 , T_2 , T_3) were of two elements, consisting of $100\mu\text{m}$, $45\mu\text{m}$, $40\mu\text{m}$ ΔE Si(SB) and 5 mm , 5 mm , 2 mm Si(Li) E detectors respectively. Typical solid angles were 1.5 msr, same for all the three telescopes. Analog signals from the detectors were processed using the standard electronics before being fed to the computer for on-line data acquisition.

The telescopes were calibrated with the radioactive ^{228}Th α -source. Typical energy resolutions (FWHM) obtained were 1.12% for T_1 and 1.13% for T_2 and T_3 respectively. The low energy cutoffs thus obtained were typically 3 MeV for proton, 5 MeV for deuteron, 5 MeV for triton and 11 MeV for α in T_1 . In T_2 and T_3 cutoffs were 1 MeV for proton, 3 MeV for deuteron, 3 MeV for triton and 7 MeV for α -particles.

Inclusive energy distributions for α -particles, proton, deuteron and triton have been measured in an angular range of 25° - 140° in case of ^7Li (47 MeV) + ^{nat}Mg reaction and in a range of 5° - 60° in case of ^{19}F (96 MeV) + ^{12}C reaction. In the centre of mass (c. m.) frame it covers up to $\sim 140^\circ$ in both the cases. Figs. 1-2 show the measured energy spectra for the light charged particles at different laboratory angles respectively for the two reactions. The shape of the energy spectra is similar for all the measured angles indicating the fact that the thermal equilibrium has been achieved in both the cases before the particle emission.

The average velocities of the observed light charged particles have been plotted in the parallel ($v_{||}$) and perpendicular (v_{\perp}) velocity plane (Figs. 3-4) for the ^7Li (47 MeV) + ^{24}Mg and ^{19}F (96 MeV) + ^{12}C reactions. It has been observed, that for all particles, the average velocities fall on a circle around the compound nucleus velocities (v_{cn}). It implies that the average velocities (as well as the average kinetic energies) of the light charged particles are independent of the centre of mass emission angles in both the reactions. It means that the energy relaxation is complete and the light charged particles are emitted from a fully equilibrated source moving with the velocity v_{cn} . At backward angles ($\theta_{lab} \geq 40^\circ$), the average velocity of the light charged particles are deviating due to large energy cutoffs in the energy spectra.

III. DISCUSSION

The experimental data have been compared with the predictions of standard statistical model calculation using the code CASCADE [14]. Figs. 5 - 8 show the centre of mass energy spectra for the various light charged particles, such as α , p, d and t, observed in the ^7Li (47 MeV) + ^{24}Mg reaction. The solid lines represent the predictions of the statistical model code

CASCADE. The optical model parameters used for calculating the transmission coefficients were taken from [16] for p , d , t , and from [15] for α -particles. The critical angular momentum for fusion, l_{cr} , is calculated using Bass model as $16\hbar$ [17]. Sharp cut-off angular momentum distribution has been assumed. In this calculation, fission has also been included as a decay channel. The radius parameter was taken to be 1.29 fm following Pühlhofer et al [14], who studied this system (i.e., ^{31}P) at lower excitation energy populated through ^{19}F (50 MeV) + ^{12}C reaction. The angular momentum dependent deformation parameters (δ_1 and δ_2 as described later) were set equal to zero. From the figures, it is observed that the theoretical predictions match well with the experimental results, indicating that all the light charged particles are evaporated from a nearly spherical ^{31}P compound nucleus. Similar behaviour have been observed for deuteron and triton also.

However, in case of ^{19}F (96 MeV) + ^{12}C reaction, the statistical model calculation using the code CASCADE, with the standard parameter set, fails (the dashed lines) to predict the shape of the experimental spectra. Figs. 9 - 12 show the observed (filled circles) and calculated (solid and dashed lines) centre of mass energy spectra for the various light charged particles emitted in the ^{19}F (96 MeV) + ^{12}C reaction. The figures indicate deviation of the experimental data from the standard statistical model predictions (dashed lines) at low as well as at high energy sides of the spectra.

According to the CASCADE calculations, the lower energy part of the spectra is controlled by the transmission probabilities to the available phase spaces. For the calculation of transmission coefficients, we have used the same sets of optical model parameters as in the case of ^7Li (47 MeV) + ^{24}Mg reaction, (i.e., the optical model parameters from [15] for alpha particles, and from [16] for proton, deuteron and triton). A deformed configuration of the compound nucleus has been assumed in the calculation. This is realized by varying only the radius parameter r_o . The optimum value of r_o is found to be ~ 1.56 fm which is consistent with our earlier work [12]. The increased radius parameter lowers the emission barrier and hence enhances the low energy yield by increasing the transmission probabilities.

The higher energy part of the spectra is controlled by the level density $\rho(E, j)$, which for a given angular momentum j and excitation energy E is defined as [14],

$$\rho(E, j) = \frac{2j+1}{12} a^{1/2} \left(\frac{\hbar^2}{2\mathcal{J}_{eff}} \right)^{3/2} \frac{1}{(E + T - \Delta - E_j)^2} \exp[2[a(E - \Delta - E_j)]^{1/2}] \quad (1)$$

where a is the level density parameter, which is taken to be $A/8$ for the present calculation, T is the thermodynamic temperature, Δ is the pairing correction, and E_j is the rotational energy which can be written in terms of the effective moment of inertia \mathcal{J}_{eff} as

$$E_j = \frac{\hbar^2}{2\mathcal{J}_{eff}} j(j+1). \quad (2a)$$

In hot rotating nuclei, formed in heavy ion reactions, the effective moment of inertia may be spin dependent and defined as,

$$\mathcal{J}_{eff} = \mathcal{J}_0 \times (1 + \delta_1 j^2 + \delta_2 j^4), \quad (2b)$$

where, the rigid body moment of inertia, \mathcal{J}_0 , is given by,

$$\mathcal{J}_0 = \frac{2}{5} A^{5/3} r_o^2. \quad (2c)$$

Here, A is the mass number and r_o is the radius parameter. Non zero values of the parameters δ_1 , δ_2 introduce spin dependence in the effective moment of inertia (Eq. 2b). The relation (Eq. 2a) defines a region in the energy, angular momentum plane (E-j plane) of allowed levels and a region where no levels occur. The region is bounded by the yrast line defined by the lowest energy state that occurs for a given angular momentum. It has been observed in the previous experiments [8,12] that the yrast line has to be modified to explain the experimental data. Different attempts have been pursued using different tools to modify the yrast line, such as, radius parameter r_o , deformation parameters δ_1 , δ_2 and the angular momentum j .

However, we have observed that the variation of a single input parameter, r_o , in the code CASCADE, is sufficient to take care of the low energy as well as the high energy side of the spectra [12]. So, in the present calculation, we varied the parameter r_o only, and kept the spin dependent parameters δ_1 , δ_2 in Eq. (2b) equal to zero, to reproduce the experimental spectra. It is clear from Figs. 9 - 12 that the calculated spectra (solid lines) agree quite well with the experimental spectra both in the low energy as well as in the high energy regions.

We have also tried to estimate the effect of entrance channel dynamics on light charged particle emission using the code HICOL [13]. Fig. 13 shows the calculated temperature of the fused nuclei as a function of time for various angular momentum values covering the range of interest for the two reactions under study. From the figure 13, it is observed that the thermal equilibration of the system is achieved, on the average within 8×10^{-22} sec after the zero time. The zero time is defined as the time when the participating nuclei begin to feel the nuclear forces and deviate from their earlier coulomb trajectories. It is also observed that the temperature decreases with increasing angular momentum. Decay time has been estimated to be $\sim 12 \times 10^{-22}$ sec, using the code PACE2, which is comparable to the formation time of the nucleus as obtained from HICOL. This implies that similar effect on particle emission should have been seen in both the reactions. However, we did not observe any such deformation effect in the ${}^7\text{Li}$ (47 MeV) + ${}^{24}\text{Mg}$ reaction. Thus the effect may not be due to the entrance channel dynamics.

Since significant yields of intermediate mass fragment have been found in the two reactions under study [18,19], it is necessary to correct the spin distribution to the fusion-evaporation channel alone which has been done in the following way. We have calculated the spin distribution for fusion-fission channel using the binary fragmentation model [19] and subtracted this part from the total spin distribution to obtain the spin distribution for the fusion-evaporation channel. The modified spin distribution has been incorporated in the statistical model calculation. It has been observed that this effect is negligible for ${}^7\text{Li}$ (47 MeV) + ${}^{24}\text{Mg}$ reaction. For

^{19}F (96 MeV) + ^{12}C reaction, it lowers the spin distribution for fusion-evaporation channel by $\sim 1\hbar$ which was not sufficient to reproduce the experimental results.

Kohlmeyer et al have measured the mass distribution of evaporation residues in ^{19}F (92 MeV) + ^{12}C reaction and have suggested a contribution from projectile breakup [20]. According to them 30% of ^{19}F was breaking up in two components, ^{15}N and ^4He . ^{15}N was then fusing with ^{12}C . If it is so, an extra fast component of α -particle was expected at the forward angles. However, we did not observe any such component in the energy and angular distribution of the α -particles. Moreover, ^7Li is expected to be more unbound against the projectile breakup and the component is expected to be more prominent in case of ^7Li (47 MeV) + ^{24}Mg reaction. But, we did not observe any such component even in case of ^7Li (47 MeV) + ^{24}Mg reaction.

Since the compound nuclei formed in ^7Li (47 MeV) + ^{nat}Mg and ^{19}F (96 MeV) + ^{12}C reactions, differ only in their input angular momentum, the deformation effect in the exit channel may be linked to the input angular momentum of the system. This conjecture has been further investigated by introducing the angular momentum dependence in the effective moment of inertia through the angular momentum dependent deformation parameters, i.e., δ_1 , δ_2 of Eq. 2b. The values of δ_1 , δ_2 have been changed to reproduce the experimental data. The best fit values thus obtained were $\delta_1 = 2.8 \times 10^{-3}$ and $\delta_2 = 2.5 \times 10^{-7}$. Theoretical predictions with the fitted parameters have been shown in Fig. 14 along with the experimental data for the α -particles emitted in the ^{19}F (96 MeV) + ^{12}C reaction. It is clear that with the above values of the δ_1 and δ_2 , the predicted spectra match well with the experimental ones. With these parameters, we have estimated an average radius parameter by averaging over the angular momentum distribution (sharp cut-off triangular distribution has been assumed, upto the critical angular momentum $21\hbar$) in the following way.

$$r_{eff}^2 = r_o^2 \frac{\sum_{o}^{j_{cr}} (1 + \delta_1 j^2 + \delta_2 j^4) (2j + 1)}{\sum_{o}^{j_{cr}} (2j + 1)} \quad (3)$$

Here, r_o is taken as 1.29 fm. j_{cr} is the critical angular momentum of the system. δ_1 and δ_2 values are as stated above. The effective radius parameter, r_{eff} , thus obtained is 1.65 fm which is within 10% of the radius parameter we have used in the statistical model calculation to reproduce the experimental data. Therefore, it can be said that the variation of single parameter r_o to fit the data is nearly equivalent to the spin dependent level density prescription as described above, at least for light compound systems involving lower spins. For such light compound systems, like ^{31}P at low spins, the present method has a distinct advantage. Here, both lower and higher energy side of the spectra could be fitted by changing a single parameter r_o , once for all. The increase of r_o causes lowering of the barrier which enhances the transmission probability, thereby correcting the lower energy side of the spectra; at the same time, it also causes a reduction of rotational energy thereby changing the level density in right direction to explain the high energy part of the spectra. On the contrary, in the standard spin dependent level density prescription, one has to take care of the low energy side of the spectra separately

by introducing a reduced barrier. As the spin dependent deformation becomes more and more significant at higher spins (as seen in Fig. 15), the present method may not lead to the realistic values of deformation parameter r_o ; and in such cases one may have to consider the spin dependent deformation only. In the case of compound nucleus ^{31}P formed in the reaction ^{7}Li (47 MeV) + ^{24}Mg , the value of l_{cr} is $\sim 16 \hbar$. It is seen from the figure 15 that the difference in the yrast lines calculated with and without angular momentum dependent deformation parameters is not quite appreciable at this angular momentum. This intuitively explains why the standard statistical model predictions have been in good agreement with the data in this case.

Finally, with the knowledge of the level densities and the transmission coefficients for the various decay modes, decay rate has been calculated for ^{19}F (96 MeV) + ^{12}C system. The rate of nucleon or cluster decay of an equilibrated compound system i to product system f is

$$R_p(E_i, j_i, E_f, j_f) dE = \rho(E_f, j_f, \pi_f) / \hbar \rho(E_i, j_i, \pi_i) \sum_{|j_f-s|}^{j_f+s} \sum_{|j_i-s|}^{j_i+s} T_l^p(\epsilon_p) dE \quad (4)$$

where $\epsilon_p = E_f - E_i - s_p$ is the particle energy, s_p is the particle separation energy and s is the spin of the particle p . j 's are the angular momentum, E 's are the excitation energies and π 's are the parities for the respective channels. ρ 's are the level density parameters as described in Eq. 1 and T_l is the transmission coefficients. Eq. 4 shows that the final shape of the spectra depends on the different decay probabilities of the nucleons and clusters from the parent nuclei i to the daughter nuclei f defined by their respective level density parameters as a function of their respective excitation energies, angular momentum and parities thus defining the complete chain of the decay cascade. However, in the present calculation, deformation has changed the relative emission of the proton and α -particles at the different stages of the decay cascade as shown in Fig. 16. In the figure, emission of α -particles and protons have been shown in first three stages of the complete decay chain by the solid and dashed curves for the radius parameters 1.29 fm and 1.56 fm respectively. The first stage correspond to the emission from ^{31}P nuclei and so the emission from the highest partial waves. The emission in the next stages has been calculated considering proper daughter nuclei populated through 1 or 2 neutron, proton, α -particle emission respectively and by adding the contributions from all those nuclei in the ratio of their respective yields. Thus first stage emission corresponds to the highest excitation energies and angular momentum whereas the second and third stages correspond to lower excitation energies and angular momentum. It is clear from the figure that inclusion of deformation enhances the proton emission a little from the highest partial waves but the lower partial wave contributions in the proton spectra does not get affected by the deformation at all. On the contrary, deformation suppressed the α -particle emission from the highest partial waves (in the first stage of the decay chain) and enhances the α -particle emission from the lower partial waves (third stage emission) considerably.

IV. SUMMARY AND CONCLUSION

We have measured the inclusive light charged particle energy spectra in an angular range of 5°-60° and 25°-140° respectively in the ^{19}F (96 MeV) + ^{12}C and ^7Li (47 MeV) + ^{nat}Mg reactions. It has been observed from the average velocity plots in the v_{\parallel} vs. v_{\perp} plane that the average velocities of all light charged particles in both the reactions stated above fall on the circles centered around their respective compound nuclear velocities, implying that these particles are emitted from equilibrated compound nuclear sources. The data in the two reactions have been compared with the statistical model calculations using the code CASCADE. It has been observed that the light charged particle spectra measured in the ^7Li (47 MeV) + ^{24}Mg reaction can be well explained in the framework of standard statistical model calculation, whereas the light charged particle spectra obtained in the ^{19}F (96 MeV) + ^{12}C reaction deviate significantly from the similar calculations. The formation times as estimated by the semiclassical calculation using the code HICOL and the decay times as estimated by PACE2 are comparable in both the cases. Therefore, the discrepancy in the light charged particle spectra obtained in the two reactions may not be solely due to the comparable formation and decay time. A satisfactory description of the measured energy spectra has been achieved by invoking a deformed configuration of the compound nucleus through the modification of the radius parameter r_0 from 1.29 fm to 1.56 fm in the statistical model calculation. Since, the two studied systems differ only in their input angular momentum distributions (for ^{19}F (96 MeV) + ^{12}C , $l_{cr}=21\hbar$ and for ^7Li (47 MeV) + ^{24}Mg , $l_{cr}=16\hbar$) the observed deformation may be due to the higher angular momentum in case of ^{19}F (96 MeV) + ^{12}C system. Incorporating the nonzero values of the angular momentum dependent deformation parameters, δ_1 and δ_2 , we could also reproduce the experimental spectra. An average radius parameter have been estimated from the fitted values of these parameters (δ_1 , δ_2) averaging over the angular momentum distribution. The average radius parameter thus obtained is 1.65 fm which is within 10% of the radius parameter we have used to reproduce the experimental data. We have shown that a modified radius parameter (r_0) alone in the statistical model calculation, may be sufficient for lighter system ($A \sim 30$) to explain a large amount of evaporative light charged particle data. However, it will be interesting to explore this simple approach in the light charged particle data for the heavier system.

ACKNOWLEDGMENTS

The authors thank the Pelletron operating staff for smooth running of the machine and Mr. D. C. Ephraim of T.I.F.R., for making the targets.

REFERENCES

- [1] I. M. Govil, R. Singh, A. Kumar, Ajay Kumar, G. Singh, S. K. Kataria and S. K. Datta, Phys. Rev. C 62, 064606 (2000).
- [2] I. M. Govil, R. Singh, A. Kumar, S. K. Datta, S. K. Kataria, Nucl. Phys. A 674, 377 (2000).
- [3] R. J. Charity, Phys. Rev. C 61, 054614 (2000).
- [4] I. M. Govil, R. Singh, A. Kumar, J. Kaur, A. K. Sinha, N. Madhavan, D. O. Kataria, P. Sugathan, S. K. Kataria, K. Kumar, Bency John and G. V. Ravi Prasad, Phys. Rev. C 57, 1269 (1998).
- [5] R. K. Choudhury, P. L. Gonthier, K. Hagel, M. N. Namboodiri, J. B. Natowitz, L. Adler, S. Simon, S. Kniffen and G. Berkowitz, Phys. Lett. 143B, 74 (1984).
- [6] G. La Rana, D. J. Moses, W. E. Parker, M. Kaplan, D. Logan, R. Lacey, J. M. Alexander and R. J. Welberry , Phys. Rev. C35, 373 (1987)
- [7] I. M. Govil, J. R. Huizenga, W. U. Schröder and J. Toke, Phys. Lett. 197B, 515 (1987).
- [8] J. R. Huizenga, A. N. Behkami, I. M. Govil, W. U. Schröder and J. Töke Phys. Rev. C40, 668 (1989)
- [9] B. Fornal, G. Viesti, G. Neibia, G. Prete and J.B. Natowitz, Phys. Rev. C 40, 664 (1989)
- [10] R. J. Charity, M. Korolija, D. G. Sarantites and L. G. Sobotka, Phys. Rev. C 56, 873 (1997)
- [11] M. N. Namboodiri, P. Gonthier, H. Ho, J. B. Natowitz, R. Eggers, L. Adler, P. Kasiraj, C. Cerruti, A. Chevarier, N. Chevarier and A. Demeyer, Nucl. Phys. A367, 313 (1981)
- [12] D. Bandyopadhyay, S. K. Basu, C. Bhattacharya, S. Bhattacharya, K. Krishan, A. Chatterjee, S. Kailas, A. Navin and A. Srivastava, Phys. Rev. C 59 1179 (1999).
- [13] H. Feldmeier, Rep. Prog. Phys. 50, 915 (1987)
- [14] F. Pühlhofer, Nucl. Phys. A280, 267 (1977)
- [15] J. R. Huizenga and G. Igo, Nucl. Phys. 29, 462(1961).
- [16] C. M. Perry and F. G. Perry, At. Data and Nucl. Data Tables 17, 1 (1976).
- [17] R. Bass, Nuclear Reactions with heavy Ions (Springer-Verlag, Berlin, 1980), p. 256.
- [18] C. Bhattacharya, D. Bandyopadhyay, S. K. Basu, S. Bhattacharya, K. Krishan, G. S. N. Murthy, A. Chatterjee, S. K. Kailas and P. Singh, Phys. Rev. C 52, 798 (1995).
- [19] C. Bhattacharya, D. Bandyopadhyay, S. K. Basu, S. Bhattacharya, K. Krishan, G. S. N. Murthy, A. Chatterjee, S. K. Kailas and P. Singh, Phys. Rev. C 54, 3099 (1996).
- [20] B. Kohlmeyer, W. Pfeffer and F. Pühlhofer Nucl. Phys. A292, 288(1977).
- [21] C. Bhattacharya, S. K. Basu, S. Bhattacharya, A. Chakraborty, S. Chattopadhyay, M. R. Dutta Majumder, K. Krishan, G. S. N. Murthy, B. Sinha, M. D. Trivedi, Y. P. Viyogi, S. K. Dutta and R. K. Bhowmik, Phys. Rev. C 44, 1049 (1991)
- [22] A. Gavron, Phys. Rev. C 21, 230 (1980)

FIGURES

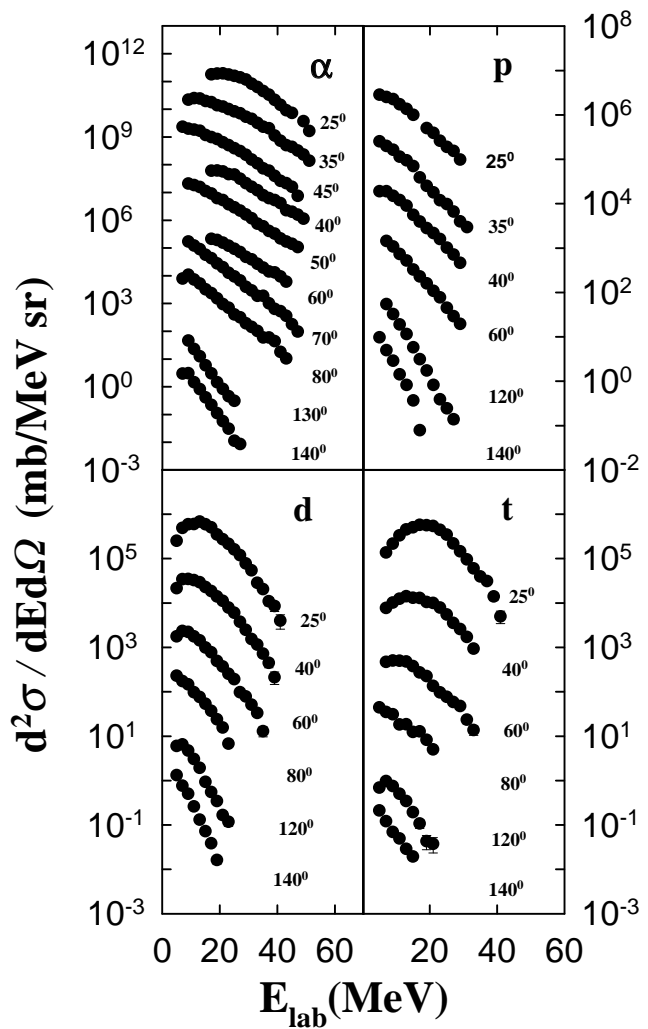


FIG. 1. inclusive (filled circles) light charged particle energy spectra obtained in the ${}^7\text{Li}$ (47 MeV) + ${}^{24}\text{Mg}$ reaction at different laboratory angles. For each curve cross-sections at highest observed angle is multiplied by 10° and the multiplication factor subsequently increases by a factor of 10 for each of the successive curve as the angle increases.

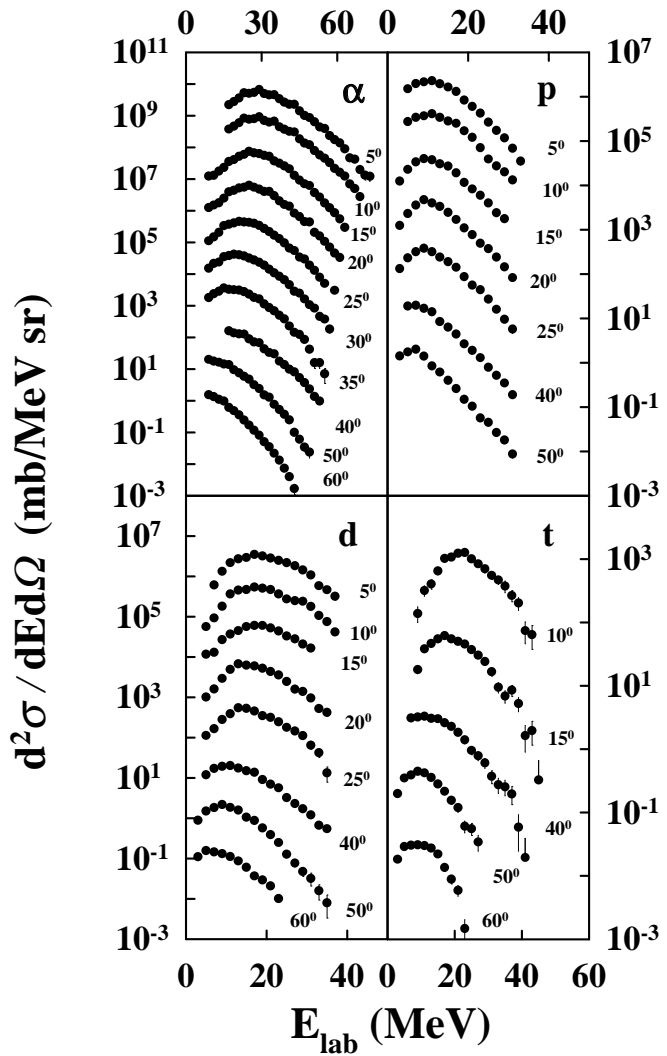


FIG. 2. Same as fig. 1 for the ^{19}F (96 MeV) + ^{12}C reaction.

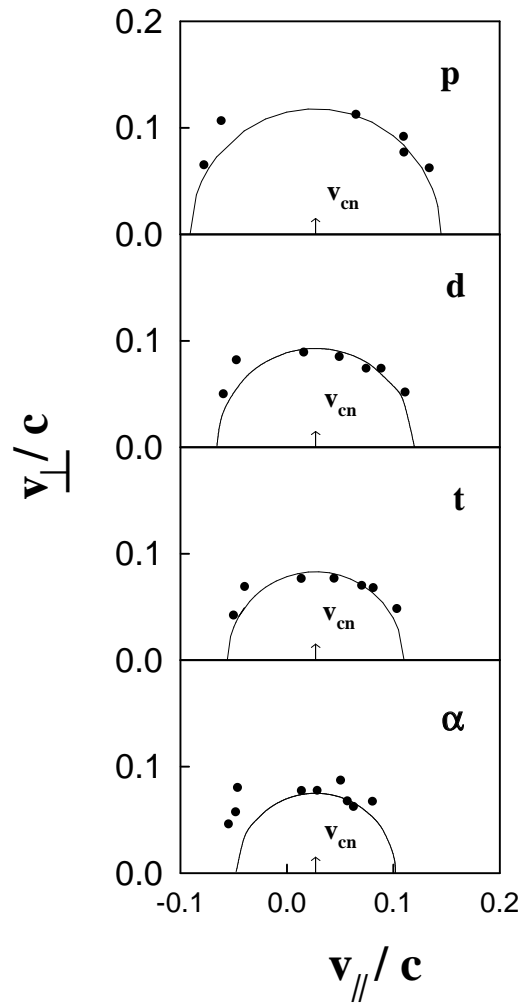


FIG. 3. Average velocities of the light charged particles, obtained in the ${}^7\text{Li}$ (47 MeV) + ${}^{24}\text{Mg}$ reaction, as a function of velocities parallel (v_{\parallel}) and perpendicular (v_{\perp}) to the beam direction. The arrow indicates the velocity of the compound nucleus.

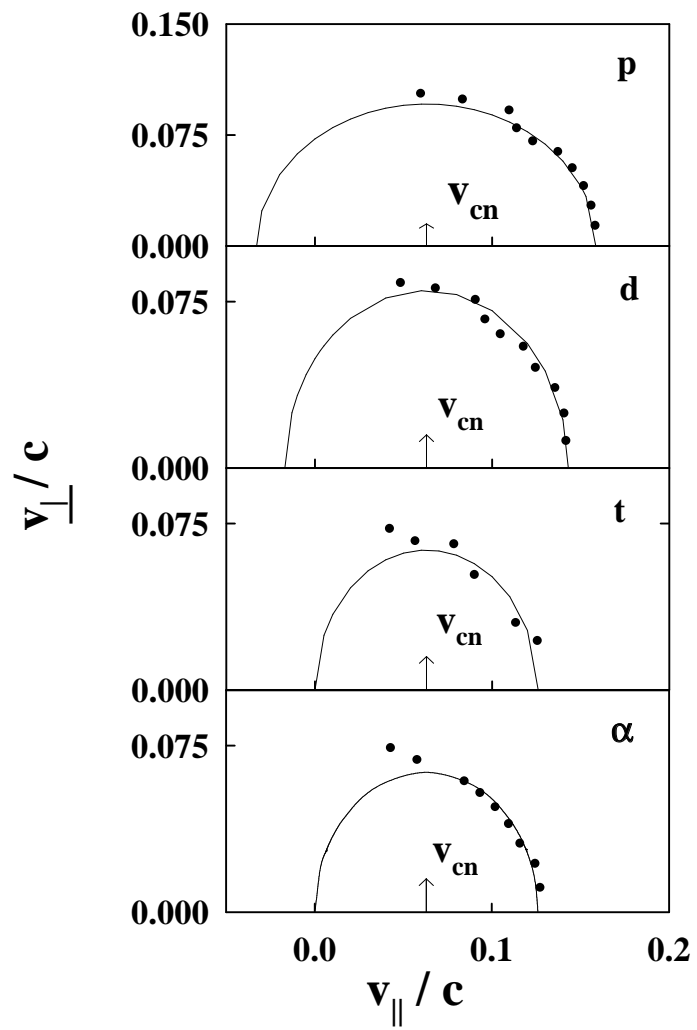


FIG. 4. Same as fig. 3 for the ^{19}F (96 MeV) + ^{12}C reaction.

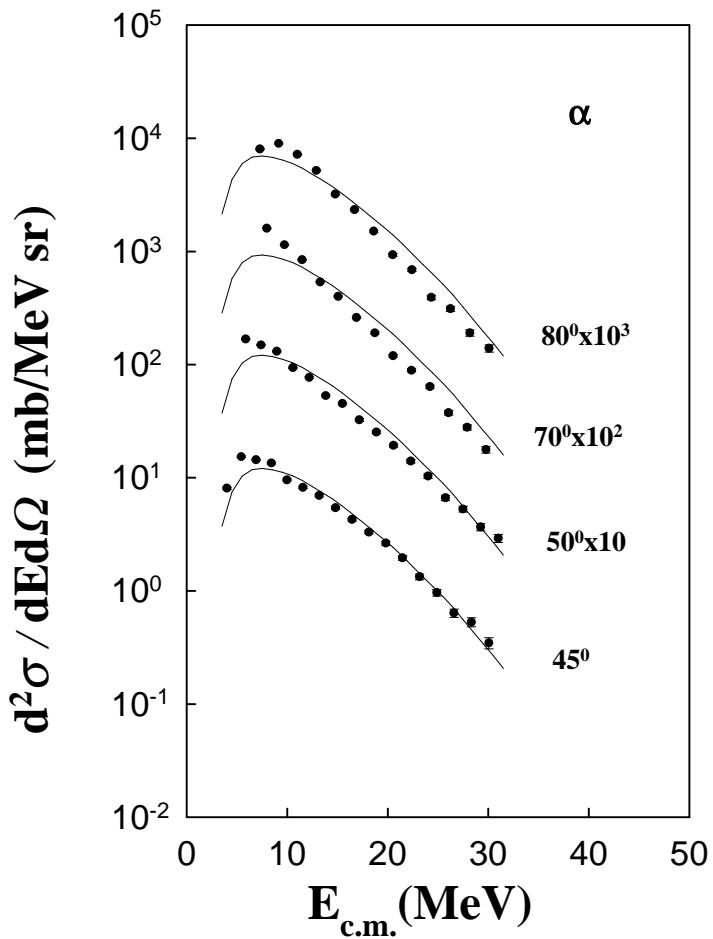


FIG. 5. inclusive (filled circles) α -particle energy spectra, obtained in the ${}^7\text{Li}$ (47 MeV) + ${}^{24}\text{Mg}$ reaction, in centre-of-mass frame measured at different laboratory angles. Solid lines (normalized at the peak of the measured data) are the prediction of CASCADE calculations with the standard value of the radius parameter, r_0 . (see text).

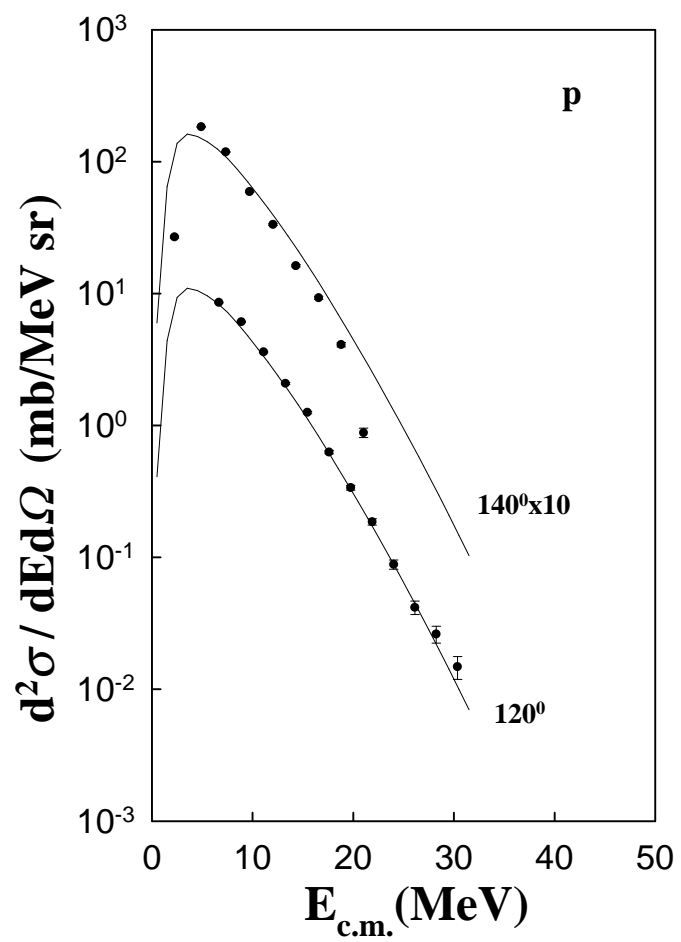


FIG. 6. Same as fig. 5 for protons.

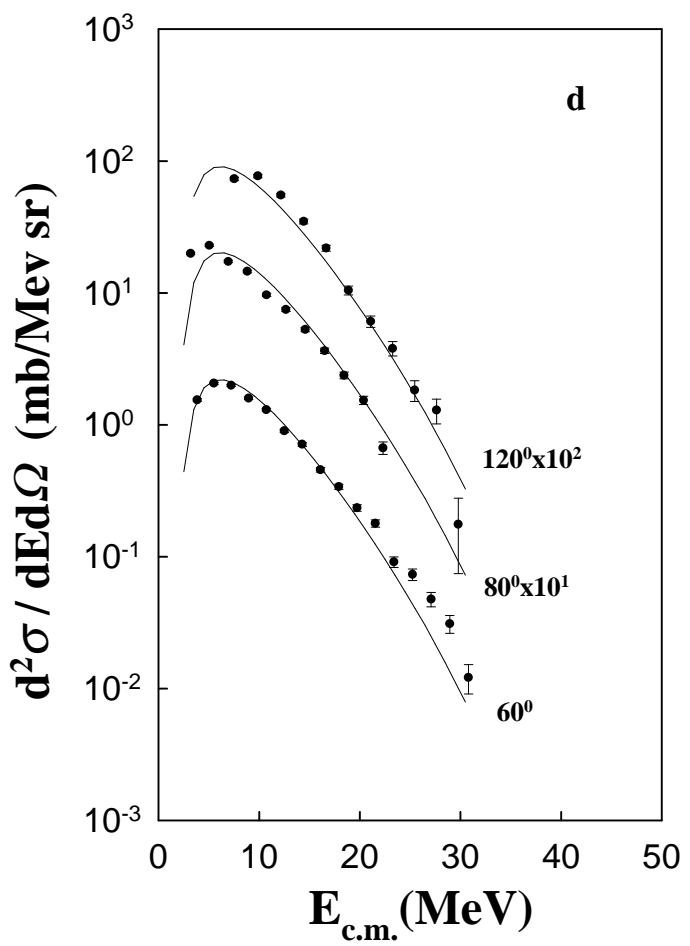


FIG. 7. Same as fig. 5 for deuterons.

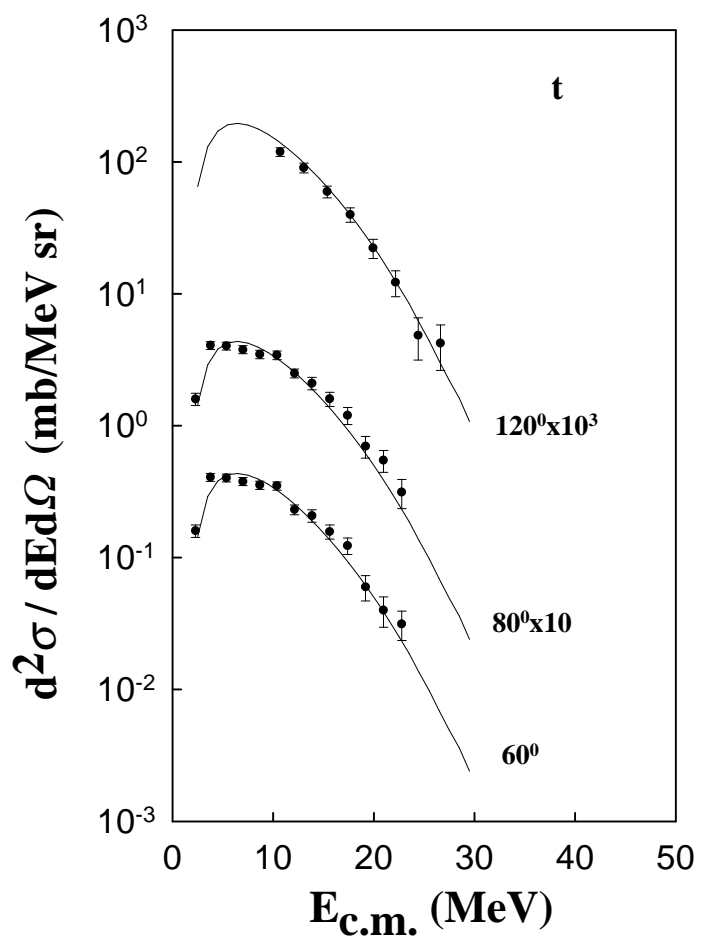


FIG. 8. Same as fig. 5 for tritons.

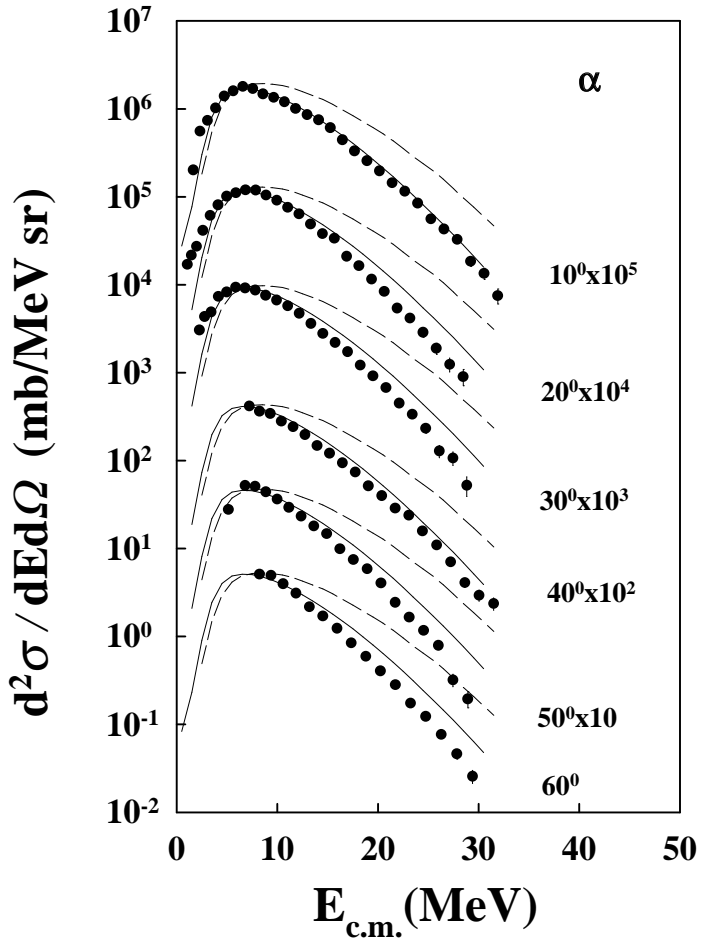


FIG. 9. inclusive (filled circles) α -particle energy spectra, obtained in the ^{19}F (96 MeV) + ^{12}C reaction, in centre-of-mass frame measured at different laboratory angles. Curves are the predictions of CASCADE calculations with the standard (dashed curves) and the modified (solid curves) values of the radius parameter, r_0 (see text). Curves are normalized at the peak of the measured data.

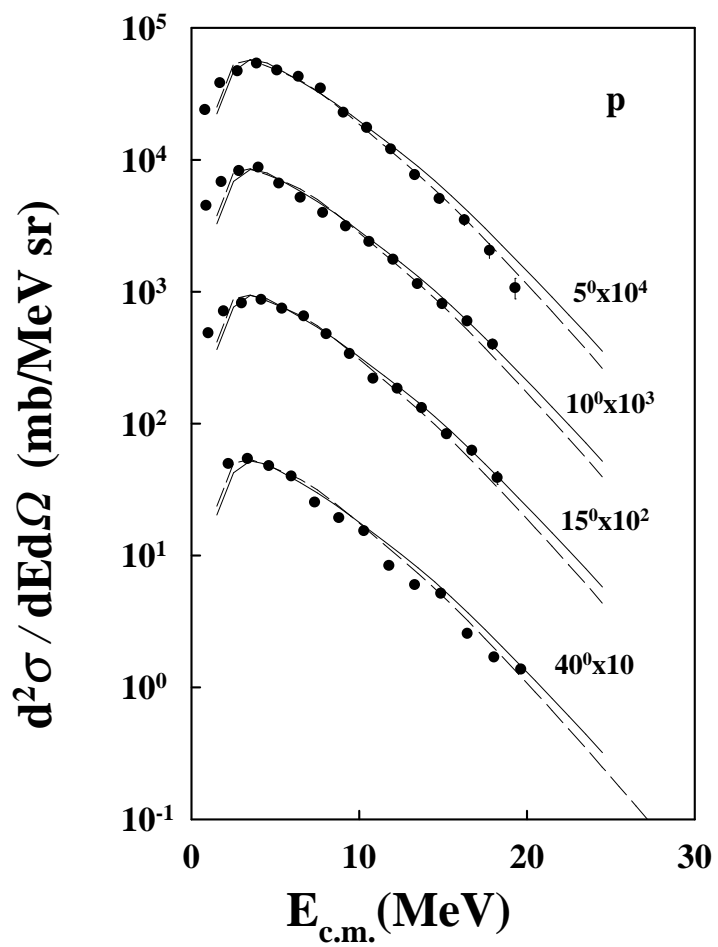


FIG. 10. Same as fig. 9 for protons.

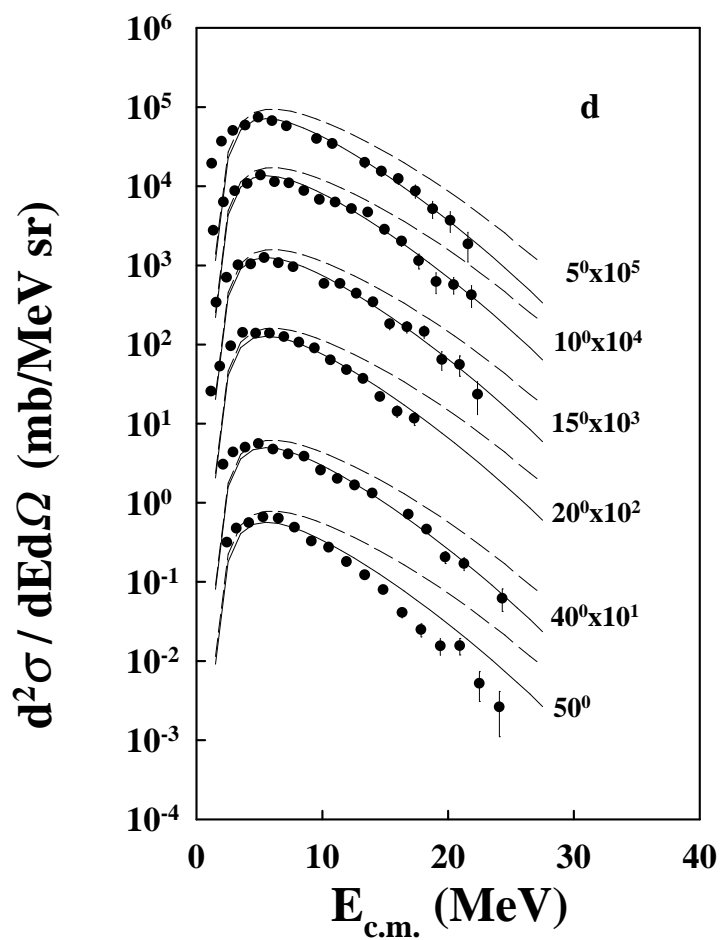


FIG. 11. Same as fig. 9 for deuterons.

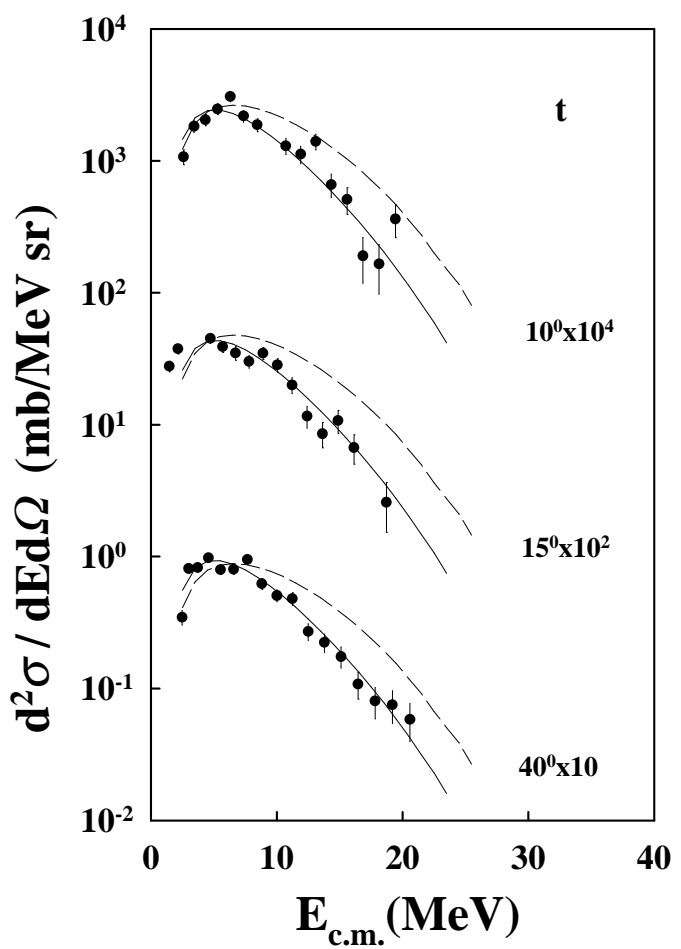


FIG. 12. Same as fig. 9 for tritons.

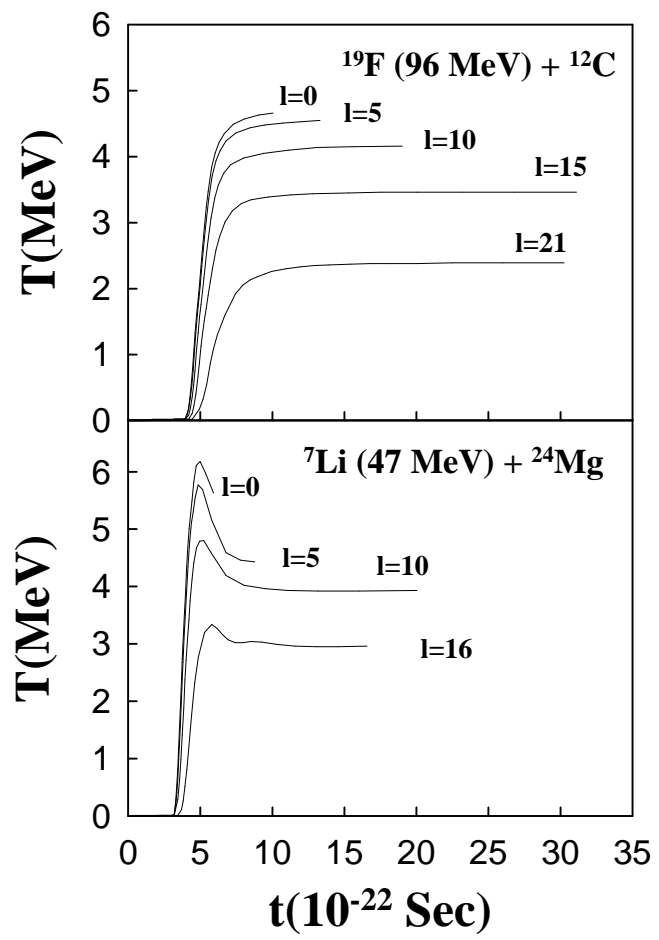


FIG. 13. Time evolution of the temperature (T) parameter as obtained from HICOL calculations for the reactions studied.

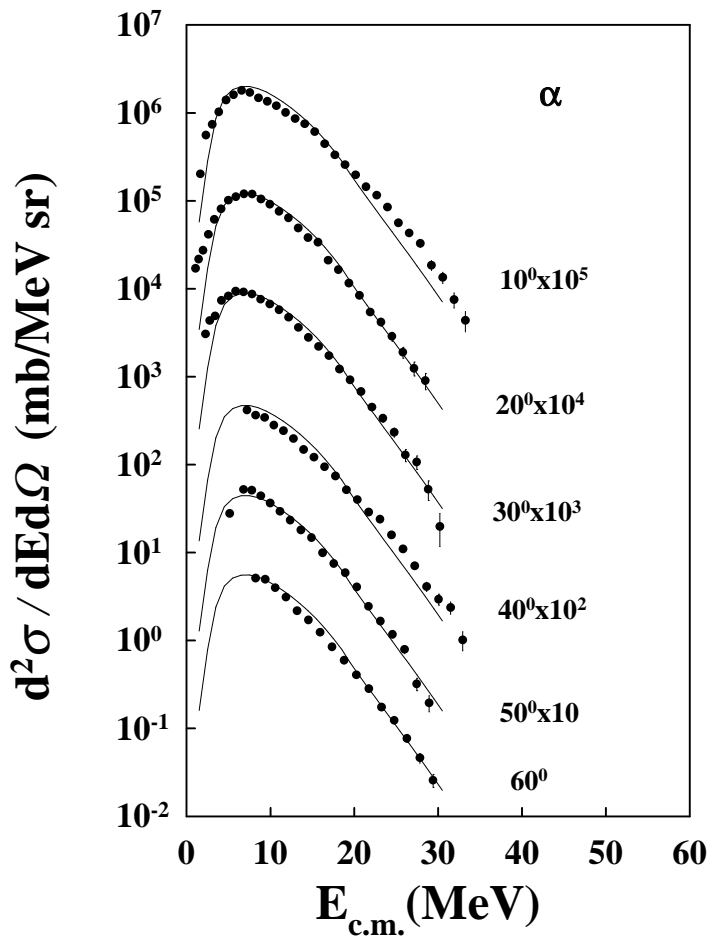


FIG. 14. Inclusive c.m. α -particle energy spectra at different laboratory angles, obtained in the ^{19}F (96 MeV) + ^{12}C reaction. Solid lines (normalized at the peak of the measured data) are the predictions of CASCADE with $\delta_1 = 2.8 \times 10^{-3}$ and $\delta_2 = 2.5 \times 10^{-7}$.

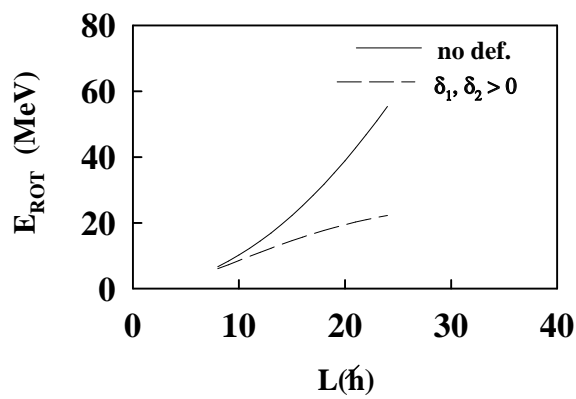


FIG. 15. Calculated yrast lines for ^{31}P nucleus with standard and modified radius parameters, for the ^{19}F (96 MeV) + ^{12}C reaction.

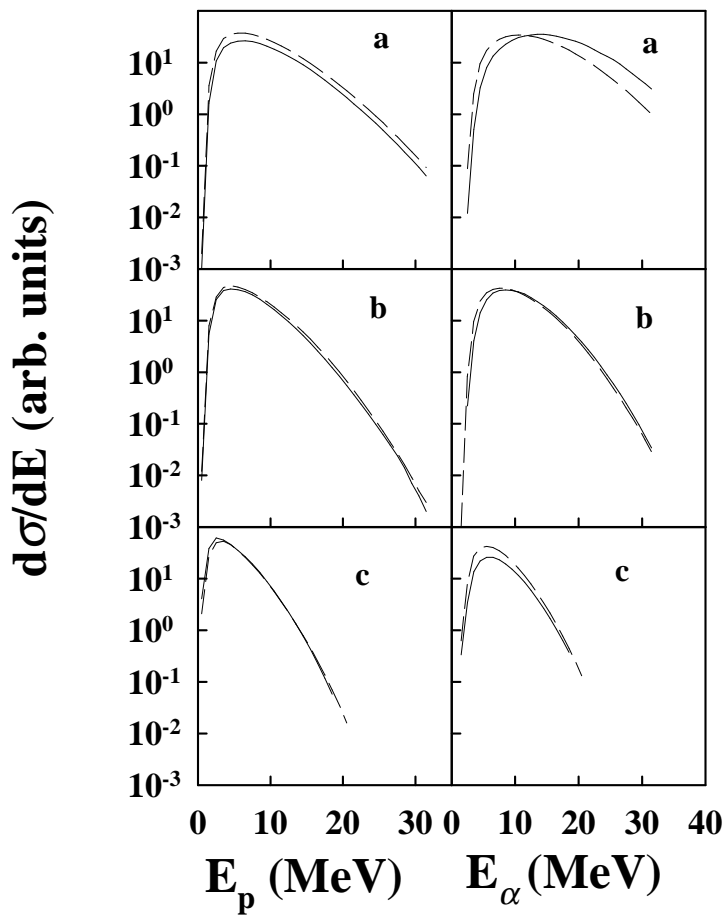


FIG. 16. Predictions of CASCADE calculation for the decay of ^{31}P nucleus, for the ^{19}F (96 MeV) + ^{12}C reaction, with the default (solid curves) and the modified (dashed curves) values of the radius parameter, r_o , for proton and α -particles at a) first stage, b) second stage and c) third stage.